

Research Article

Highly Dispersed Re-Doped CoAl_2O_4 Nanopigments: Synthesis and Chromatic Properties

Yuping Tong, Hailong Zhang, Shun Wang, Zheng Chen, and Baixue Bian

School of Civil Engineering and Communication, North China University of Water Resources and Electric Power, Zhengzhou 450011, China

Correspondence should be addressed to Yuping Tong; tongqzm@163.com

Received 16 December 2015; Revised 8 February 2016; Accepted 16 February 2016

Academic Editor: William Yu

Copyright © 2016 Yuping Tong et al. This is an open access article distributed under the Creative Commons Attribution License, which permits unrestricted use, distribution, and reproduction in any medium, provided the original work is properly cited.

Nanosized spinel $\text{CoAl}_{2-x}\text{Re}_x\text{O}_4$ complex oxides were prepared by self-propagation combustion method. The products have been characterized by XRD, SEM, and EDS. The results indicated that Al^{3+} can be partly replaced by Re^{3+} when the doped amount is less than 10%, which forms single solid solution. The NIR reflectance and chromatic properties of samples have also been investigated. The substitution of Re^{3+} for Al^{3+} in CoAl_2O_4 can increase the blueness of pigments. SEM results revealed that the obtained $\text{CoAl}_{2-x}\text{Re}_x\text{O}_4$ pigments consisted of highly dispersed spherical-like nanoparticles with uniform size distribution. EDS results indicated that the distribution of element was considerably uniform with no chemical segregation phenomenon.

1. Introduction

Spinel-type structure pigments with a general formula $\text{A}_2\text{B}_2\text{O}_4$ have attracted extensive attention due to their chemical and thermal stability, which have been applied in decorating porcelains, ceramics, catalysts, paints, and so forth [1–3]. Among them, CoAl_2O_4 is one of the most important blue pigments, which has classic spinel-type structure and superior properties, such as high resistance to acids, and chemical, color, optical, and thermal stabilities [4–6]. Particularly, for application as optical devices like color filters or pigments, the presence of highly dispersed submicrometer or nano- CoAl_2O_4 particles is important and indispensable [7].

Recent efforts have focused on tailoring a controllable and simple synthetic method for high-quality CoAl_2O_4 nanopigment. Many new synthetic technologies have been developed to synthesize CoAl_2O_4 nanopigment, such as organic ligand-assisted supercritical water hydrothermal method [8], polyacrylamide gel method [9], coprecipitation process [6], sol-gel method [5, 10], autoignition technique [11], molten salts method [12], and combustion method [13].

The self-propagation combustion method has been developed by our team for preparation of pyrochlore-type and spinel-type nanoparticles [14, 15]. In this paper, we study

synthesis and chromatics properties of rare earth ion doped CoAl_2O_4 nanopigment via self-propagation combustion method, based on the fact that rare earth element as doping ion can change the crystal structure and play an important role in stabilizing the color and changing the color of pigments.

2. Experimental

2.1. Preparation of Materials. All reagents were of analytical grade and used without further purification. In this work, all pigment samples of $\text{CoAl}_{2-x}\text{Re}_x\text{O}_4$ ($\text{Re} = \text{Y, La, Nd, Sm, and Eu}$) were synthesized by self-propagation combustion method. $\text{Co}(\text{NO}_3)_2 \cdot 6\text{H}_2\text{O}$ and $\text{Al}(\text{NO}_3)_3 \cdot 9\text{H}_2\text{O}$ were used as the precursors of Co and Al, respectively. $\text{Re}(\text{NO}_3)_3 \cdot n\text{H}_2\text{O}$ was obtained by dissolving Re_2O_3 in concentrated HNO_3 . Urea was used as fuel. According to the formula $\text{CoAl}_{2-x}\text{Re}_x\text{O}_4$ (where $x = 0.05, 0.1, 0.15, 0.2, \text{ and } 0.3$), stoichiometric amounts of $\text{Co}(\text{NO}_3)_2 \cdot 6\text{H}_2\text{O}$, $\text{Al}(\text{NO}_3)_3 \cdot 9\text{H}_2\text{O}$, and $\text{Re}(\text{NO}_3)_3 \cdot n\text{H}_2\text{O}$ were added to urea aqueous solution in turn. After a series of steps of magnetic force stirring, evaporating, and self-propagating combustion, the loose precursor was obtained. The precursor was ground into powder and then submitted to calcination at 750°C

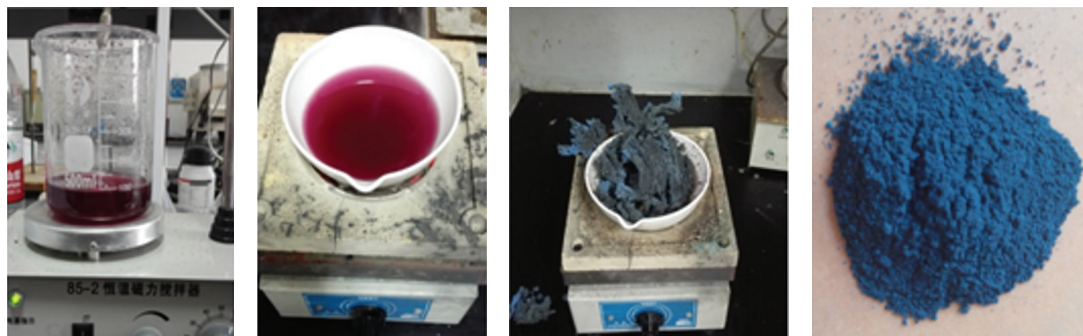


FIGURE 1: The synthesis procedure of CoAl_2O_4 nanoparticles.

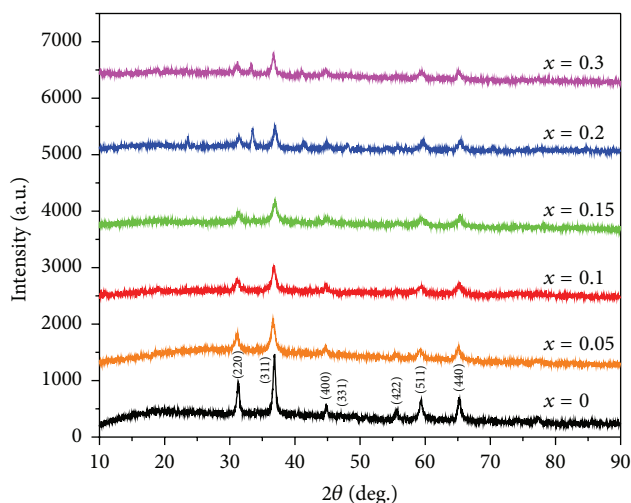


FIGURE 2: XRD patterns of $\text{CoAl}_{2-x}\text{La}_x\text{O}_4$ ($x = 0, 0.05, 0.1, 0.2$, and 0.3) precursor calcined at 750°C for 4 h.

for 4 h. The synthesis procedure and product of CoAl_2O_4 nanoparticles are shown in Figure 1.

2.2. Instrumentation. The crystalline phase structure was determined by Bruker D8 Advance X-ray diffractometer (XRD) using $\text{Cu K}\alpha$ radiation. Scanning electron microscopy (SEM) image was recorded on a JSM-7500F scanning electron microscope, and EDS was taken on INCA PentaFET-x3 energy dispersive X-ray detector. The CIE 1976 $L^*a^*b^*$ colorimetric method was used, as recommended by the Commission Internationale de l'Eclairage (CIE). In this method, L^* is the lightness axis [black (0) to white (100)], a^* is the green (–value) to red (+value) axis, and b^* is the blue (–value) to yellow (+value) axis. The parameter C^* (chroma) represents saturation of the color. For each colorimetric parameter of a sample, measurements were made in triplicate and an average value was chosen as the result. Typically, for a given sample, the standard deviation of the measured CIE- $L^*a^*b^*$ values is less than 0.10, and the relative standard deviation is not higher than 1%, indicating that the measurement error can be ignored. UV-vis-NIR reflectance of the obtained pigments was carried out by UV-vis-NIR spectrophotometer (Perkin Elmer Lambda 950), using polytetrafluoroethylene as a white standard.

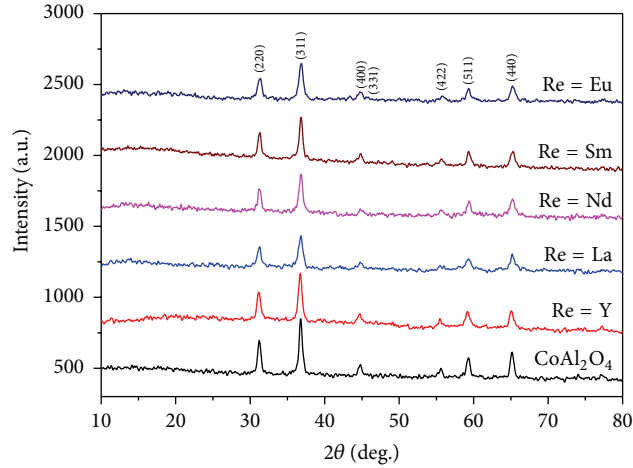
3. Results and Discussions

3.1. XRD Analysis. The XRD patterns of $\text{CoAl}_{2-x}\text{La}_x\text{O}_4$ ($x = 0, 0.05, 0.1, 0.2$, and 0.3) nanocrystals are shown in Figure 2. From Figure 2, it is clear that all the main peaks when $x < 0.2$ are similar except for a trivial difference of 2θ value. All diffraction peaks of $\text{CoAl}_{2-x}\text{La}_x\text{O}_4$ ($x < 0.2$) are in good agreement with the reflection of spinel CoAl_2O_4 phase (JCPDS number 44-016) which indicates that Al ion can be replaced by La^{3+} and the crystal type remains unchanged with the structure of CoAl_2O_4 only with small crystal distortion. In our present investigation, we found that another phase evolution starts from that composition ($x = 0.2$) onwards. The diffraction peaks at $2\theta = 25.51^\circ$ and 34.03° when $x \geq 0.2$ are indexed as LaAlO_3 , which indicates that more La cannot be accommodated in CoAl_2O_4 . Moreover, compared with pure CoAl_2O_4 , the diffraction peaks of doped products become low. The obtained CoAl_2O_4 nanocrystals at 750°C have higher crystallinity than that of products via polyacrylamide gel method at the same temperature [9].

For $\text{CoAl}_{1.95}\text{Re}_{0.05}\text{O}_4$ nanocrystallines, we study the effect of the different doped ion on the structure of products. The XRD patterns of $\text{CoAl}_{1.95}\text{Re}_{0.05}\text{O}_4$ ($\text{Re} = \text{Y, La, Nd, Sm, and Eu}$) precursor calcined at 750°C for 4 h are shown in Figure 3.

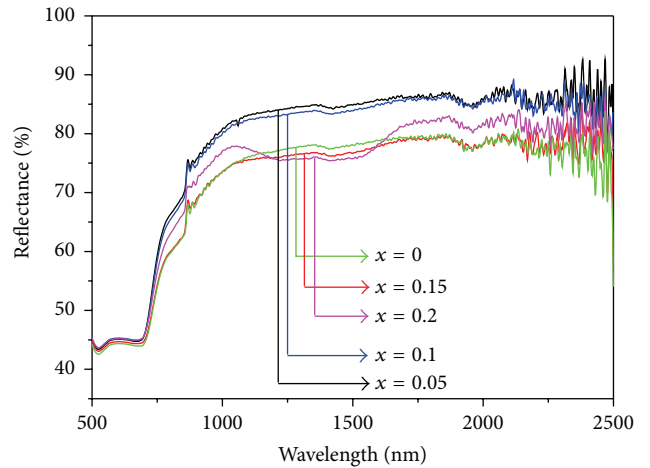
TABLE 1: Lattice constant and crystal size of CoAl_2O_4 and $\text{CoAl}_{1.95}\text{Re}_{0.05}\text{O}_4$.

Sample	Lattice constant a	Crystal size/nm	Strain/%	Radius/ Re^{3+}
CoAl_2O_4	8.09881	18.4	-0.081	$R(\text{Al}^{3+}) = 0.54$
$\text{CoAl}_{1.95}\text{Y}_{0.05}\text{O}_4$	8.09550	12.8	-0.094	1.02
$\text{CoAl}_{1.95}\text{La}_{0.05}\text{O}_4$	8.09297	10.3	-0.426	1.18
$\text{CoAl}_{1.95}\text{Nd}_{0.05}\text{O}_4$	8.09050	8.9	-0.591	N/A
$\text{CoAl}_{1.95}\text{Sm}_{0.05}\text{O}_4$	8.08787	11.6	-0.419	1.08
$\text{CoAl}_{1.95}\text{Eu}_{0.05}\text{O}_4$	8.08547	11	-0.125	1.07

FIGURE 3: XRD patterns of CoAl_2O_4 and $\text{CoAl}_{1.95}\text{Re}_{0.05}\text{O}_4$ ($\text{Re} = \text{Y}, \text{La}, \text{Nd}, \text{Sm}, \text{and Eu}$).

It can be found from Figure 3 that all the main diffraction peaks are similar and belong to the standard spinel phase of CoAl_2O_4 . The lattice constants of samples are obtained by Jade 6 program, the average crystal sizes are determined from the XRD patterns according to the Scherrer equation, and corresponding data are listed in Table 1. The average crystal size is about 8~20 nm. From the XRD patterns, it could be noted that doping of CoAl_2O_4 with Re^{3+} leads to a marginal shift of diffraction peaks towards lower 2θ angle side only except for the doping of La^{3+} . Due to larger radius of Y^{3+} , Eu^{3+} , Sm^{3+} , Nd^{3+} , and La^{3+} , the lattice constant value has been decreased from 8.09550 to 8.08547.

3.2. NIR Reflectance of Samples. Figure 4 shows the NIR reflectance spectra of the pigments. The sample of CoAl_2O_4 , $\text{CoAl}_{1.95}\text{Eu}_{0.05}\text{O}_4$, $\text{CoAl}_{1.9}\text{Eu}_{0.1}\text{O}_4$, $\text{CoAl}_{1.85}\text{Eu}_{0.15}\text{O}_4$, and $\text{CoAl}_{1.8}\text{Eu}_{0.2}\text{O}_4$ processes the NIR reflectance of about 79.7%, 86.5%, 85.8%, 79.4%, and 82.8%, respectively. It can be seen that the presence of Eu in CoAl_2O_4 improves the NIR reflectance to some extent except for $\text{CoAl}_{1.85}\text{Eu}_{0.15}\text{O}_4$. The sample $\text{CoAl}_{1.95}\text{Eu}_{0.05}\text{O}_4$ processes the highest NIR reflectance and enhances the NIR reflectance to 86.5%. With the increasing of Eu-doped amount, the NIR reflectance decreases, which may be due to similar results to “fluorescence quenching.”

FIGURE 4: NIR reflectance of $\text{CoAl}_{2-x}\text{Eu}_x\text{O}_4$ samples.

3.3. Chromatic Properties of Samples. Based on the above discussion, for $\text{CoAl}_{1.95}\text{Re}_{0.05}\text{O}_4$, we study the chromatic properties of the obtained $\text{CoAl}_{1.95}\text{Re}_{0.05}\text{O}_4$ pigment samples, which can be assessed from their CIE 1976 $L^*a^*b^*$ color coordinate values; the corresponding values are shown in Table 2. With the doping of Re^{3+} , the increasing of b^* value

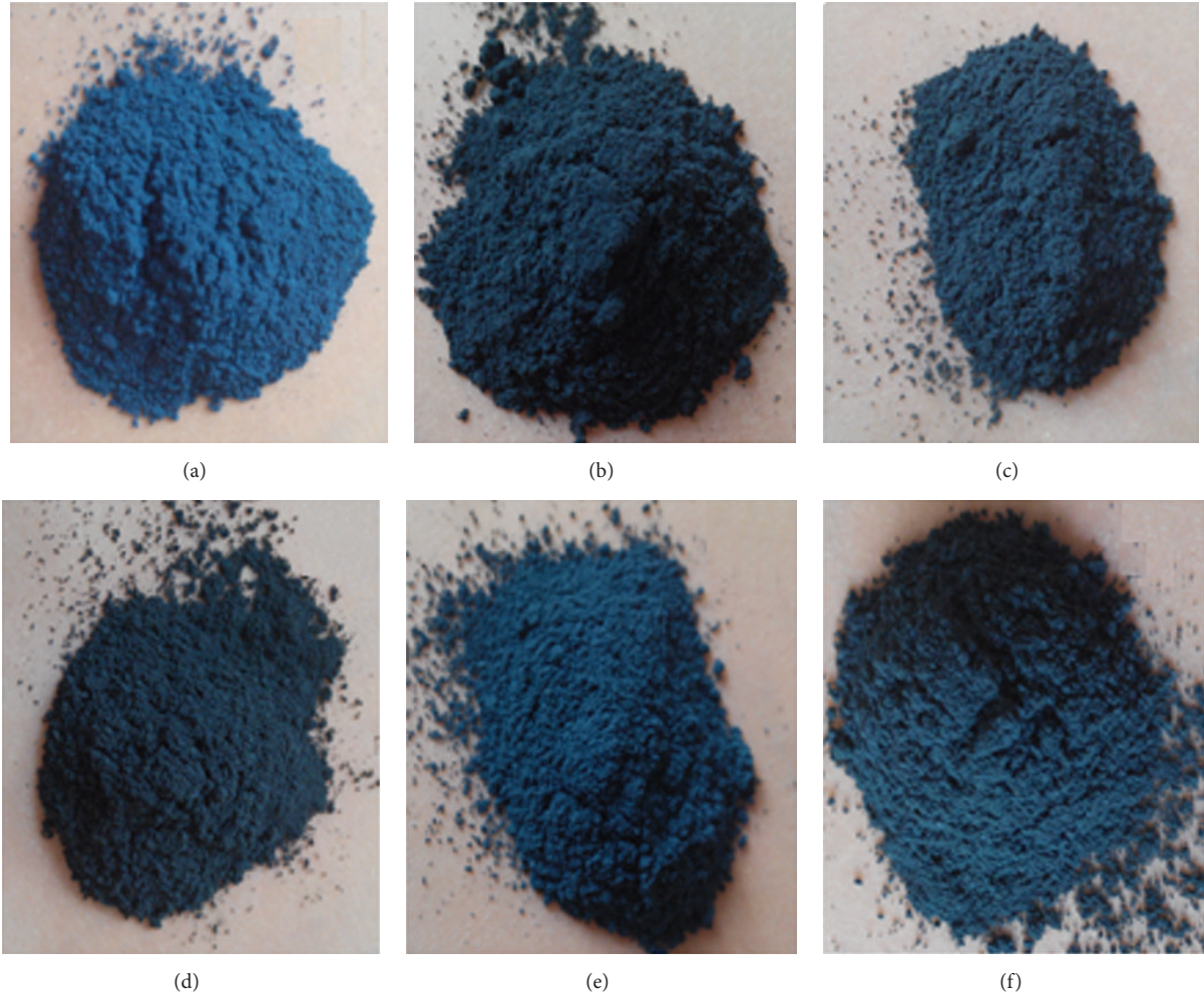


FIGURE 5: Photographs of CoAl_2O_4 and $\text{CoAl}_{1.95}\text{Re}_{0.05}\text{O}_4$ ($\text{Re} = \text{Y, La, Nd, Sm, and Eu}$) pigments.

from -23.9 to -76.5 also presents the enhancement of the blueness of pigments, comparing with undoped samples. At the same time, L^* value decreases from 34.8 to 20.3 in the presence of Re^{3+} , which indicates that the darkness increases. This result is in agreement with the change of color of the pigments from bright blue to dark blue and then to light blue (Figure 5). It can be concluded that the doping of Re^{3+} can improve the blueness of pigments. To the best of our knowledge, for cobalt-based pigments, the Co^{2+} ions can be incorporated as coloring in all kinds of ceramics and enamels where they adopt the tetrahedral coordination. When Al^{3+} is replaced by Re^{3+} with larger radius, crystal lattice distortion appears, which may result in the shift of Co^{2+} from tetrahedral coordination to octahedral one and then cause the change of color. Combining NIR reflectance results with chromatic data, $\text{CoAl}_{1.95}\text{Eu}_{0.05}\text{O}_4$ should be a good candidate as a “colored cool pigment” for use in the surface coating application.

3.4. SEM and EDS Analysis. The representative SEM images of the obtained pigments are shown in Figure 6. As can be

TABLE 2: Color coordinates of the CoAl_2O_4 and $\text{CoAl}_{1.95}\text{Re}_{0.05}\text{O}_4$ powder pigments.

Pigment composition	Color coordinates		
	L^*	a^*	b^*
CoAl_2O_4	34.8	14.7	-23.9
$\text{CoAl}_{1.95}\text{Y}_{0.05}\text{O}_4$	20.8	41.3	-76.5
$\text{CoAl}_{1.95}\text{La}_{0.05}\text{O}_4$	21.9	-4.42	-7.64
$\text{CoAl}_{1.95}\text{Nd}_{0.05}\text{O}_4$	26.1	27.3	-74.2
$\text{CoAl}_{1.95}\text{Sm}_{0.05}\text{O}_4$	20.3	21.6	-75.3
$\text{CoAl}_{1.95}\text{Eu}_{0.05}\text{O}_4$	24.2	25.8	-58.6

seen, the CoAl_2O_4 powders (Figure 6(a)) have sphere-like structure with the size of 20 nm , but to some extent, the particles are a bit aggregated. However, the dispersibility of samples is still better than that of samples obtained by sol-gel precursor. Many researchers reported quasi-spheric or platy or irregular shapes for CoAl_2O_4 powders prepared by soft-chemical methods, and so forth [5, 9]. By La doped into CoAl_2O_4 (Figure 6(b)), it can be seen that the products are

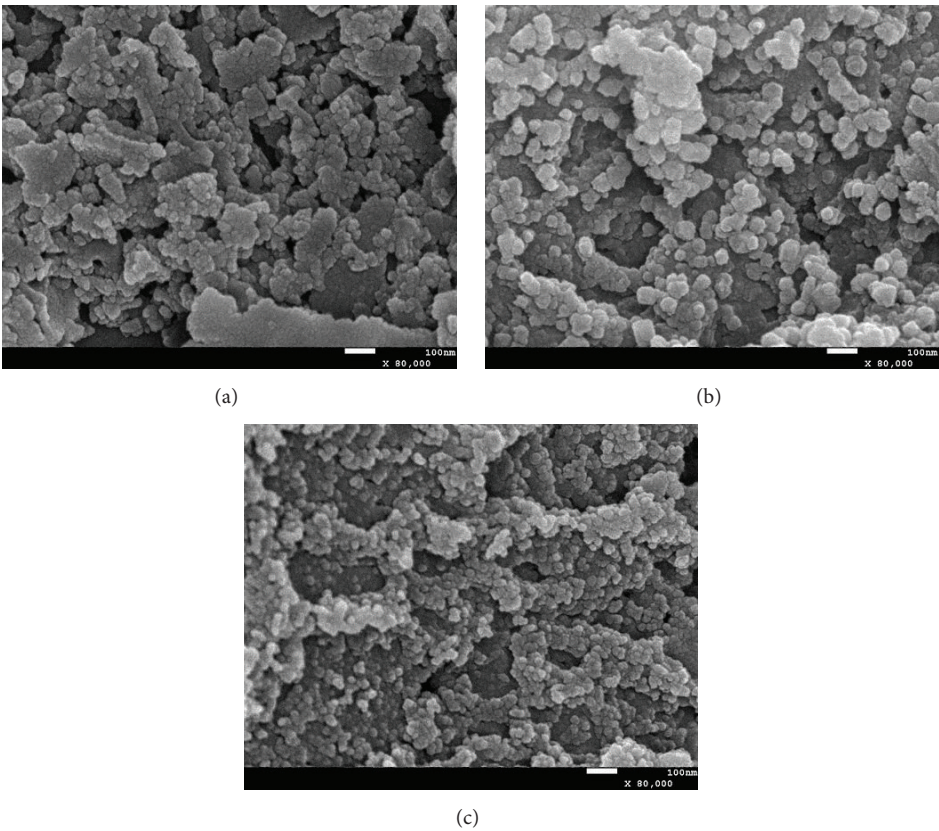


FIGURE 6: SEM images of samples: (a) CoAl_2O_4 , (b) $\text{CoAl}_{1.85}\text{La}_{0.15}\text{O}_4$, and (c) $\text{CoAl}_{1.9}\text{Eu}_{0.1}\text{O}_4$.

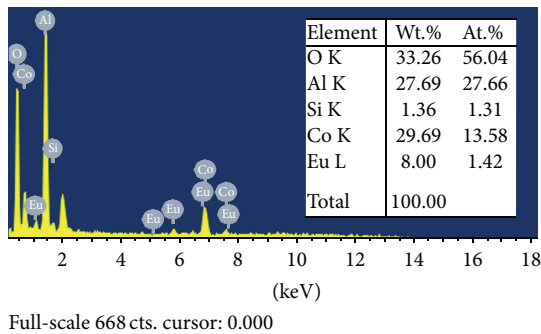


FIGURE 7: EDS results of $\text{CoAl}_{1.9}\text{Eu}_{0.1}\text{O}_4$ nanocrystals.

composed of highly dispersed nanoparticles with the size of 30 nm. Figure 6(c) shows that the $\text{CoAl}_{1.85}\text{Eu}_{0.15}\text{O}_4$ samples also consist of well-dispersed uniform nanoparticles. The results reveal that Re-doped CoAl_2O_4 samples have good dispersibility and uniform size distribution.

Figure 7 gives the EDS results of $\text{CoAl}_{1.9}\text{Eu}_{0.1}\text{O}_4$ samples. It is clear that $\text{CoAl}_{1.9}\text{Eu}_{0.1}\text{O}_4$ nanocrystals are made up of O, Al, Co, Eu, and Si. The ratio $\text{Co} : (\text{Al} + \text{Eu})$ is approximately equal to 1:2, and $\text{Al} : \text{Eu} \approx 19:1$, which gives stoichiometric formula of the as-obtained product $\text{CoAl}_{1.9}\text{Eu}_{0.1}\text{O}_4$ with no chemical segregation phenomenon. The Si peak in the spectrum is from the silicon chip for making the sample. From the surface scanning results (Figure 8), it can be seen that

the distribution of O, Al, Co, and Eu element is considerably uniform.

4. Conclusions

A series of Re-doped CoAl_2O_4 nanosized blue pigments have been synthesized. XRD results indicated that CoAl_2O_4 had limited accommodation for Re^{3+} only when $x < 0.2$. When $x \geq 0.2$ in $\text{CoAl}_{2-x}\text{Re}_x\text{O}_4$, the impurity phase will be formed. It can be concluded from the chromatic data that the doping of Re^{3+} can improve the blueness of pigments. SEM images revealed that the doped samples had good dispersibility and uniform size distribution. Combining NIR reflectance results

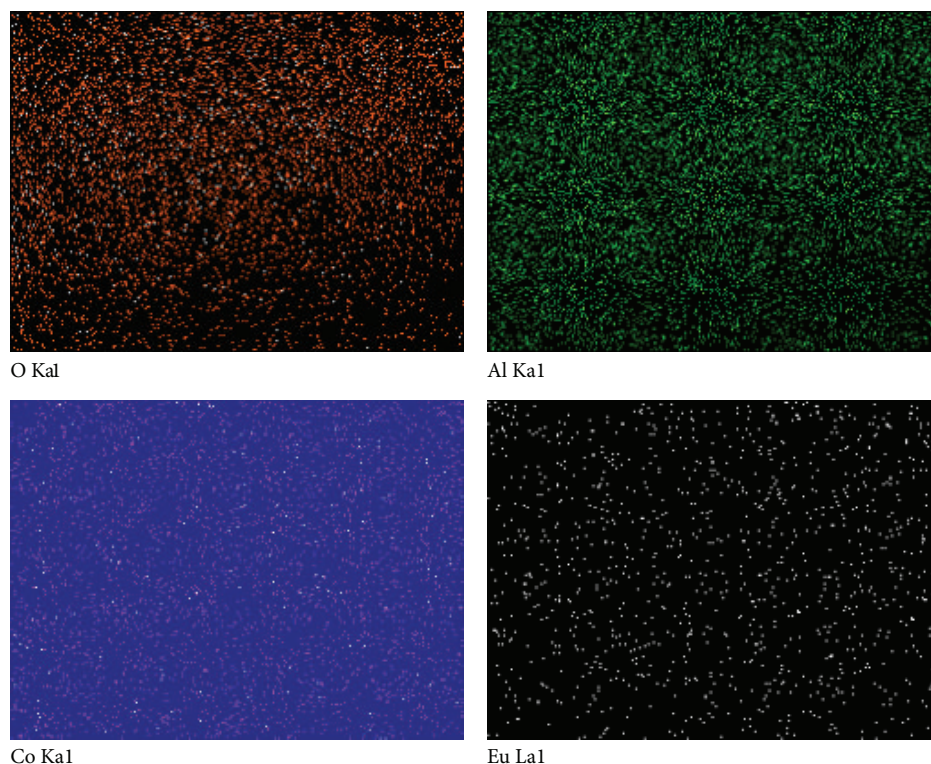


FIGURE 8: Surface scanning images of $\text{CoAl}_{1.9}\text{Eu}_{0.1}\text{O}_4$ nanocrystals.

with chromatic data, $\text{CoAl}_{1.95}\text{Eu}_{0.05}\text{O}_4$ can be considered as a good “colored cool pigment” candidate for use in the surface coating application.

Competing Interests

The authors declare that there are no competing interests regarding the publication of this paper.

Acknowledgments

The authors gratefully acknowledge the financial support of Key Programs for Science and Technology Development of Henan Province, China (no. 122102210239), the Fund for Young Teachers in University of Henan Province, China (2012GGJS-103), the Key Science and Technology Plan Projects of Zhengzhou City (no. 131PPTGG410-12), and the Natural Science Research Projects of Education Department of Henan Province, China (13B560115).

References

- [1] I. H. Gul, A. Maqsood, M. Naeem, and M. N. Ashiq, “Optical, magnetic and electrical investigation of cobalt ferrite nanoparticles synthesized by co-precipitation route,” *Journal of Alloys and Compounds*, vol. 507, no. 1, pp. 201–206, 2010.
- [2] M. Salavati-Niasari and F. Davar, “Synthesis of copper and copper(I) oxide nanoparticles by thermal decomposition of a new precursor,” *Materials Letters*, vol. 63, no. 3-4, pp. 441–443, 2009.
- [3] J. Alarcon, P. Escibano, and R. M. Marín, “Co(II) based ceramic pigments,” *British Ceramic Transactions*, vol. 84, no. 5, pp. 170–172, 1985.
- [4] S. Akdemir, E. Ozel, and E. Suvaci, “Solubility of blue CoAl_2O_4 ceramic pigments in water and diethylene glycol media,” *Ceramics International*, vol. 37, no. 3, pp. 863–870, 2011.
- [5] X. L. Duan, M. Pan, F. P. Yu, and D. R. Yuan, “Synthesis, structure and optical properties of CoAl_2O_4 spinel nanocrystals,” *Journal of Alloys and Compounds*, vol. 509, no. 3, pp. 1079–1083, 2011.
- [6] M. Peymannia, A. Soleimani-Gorgani, M. Ghahari, and F. Najafi, “Production of a stable and homogeneous colloid dispersion of nano CoAl_2O_4 pigment for ceramic ink-jet ink,” *Journal of the European Ceramic Society*, vol. 34, no. 12, pp. 3119–3126, 2014.
- [7] J. Merikhi, H.-O. Jungk, and C. Feldmann, “Sub-micrometer CoAl_2O_4 pigment particles-synthesis and preparation of coatings,” *Journal of Materials Chemistry*, vol. 10, no. 6, pp. 1311–1314, 2000.
- [8] D. Rangappa, T. Naka, A. Kondo, M. Ishii, T. Kobayashi, and T. Adschiri, “Transparent CoAl_2O_4 hybrid nano pigment by organic ligand-assisted supercritical water,” *Journal of the American Chemical Society*, vol. 129, no. 36, pp. 11061–11066, 2007.
- [9] M. Jafari and S. A. Hassanzadeh-Tabrizi, “Preparation of CoAl_2O_4 nanoblue pigment via polyacrylamide gel method,” *Powder Technology*, vol. 266, pp. 236–239, 2014.
- [10] M. Salavati-Niasari, M. Farhadi-Khouzani, and F. Davar, “Bright blue pigment CoAl_2O_4 nanocrystals prepared by modified sol-gel method,” *Journal of Sol-Gel Science and Technology*, vol. 52, no. 3, pp. 321–327, 2009.

- [11] S. Salem, "Relationship between gel rheology and specific surface area of nano-sized CoAl_2O_4 powder manufactured by autoignition technique," *Materials Letters*, vol. 139, pp. 498–500, 2015.
- [12] N. Ouahdi, S. Guillemet, J. J. Demai et al., "Investigation of the reactivity of AlCl_3 and CoCl_2 toward molten alkali-metal nitrates in order to synthesize CoAl_2O_4 ," *Materials Letters*, vol. 59, no. 2-3, pp. 334–340, 2005.
- [13] I. S. Ahmed, "A simple route to synthesis and characterization of CoAl_2O_4 nanocrystalline via combustion method using egg white (ovalbumine) as a new fuel," *Materials Research Bulletin*, vol. 46, no. 12, pp. 2548–2553, 2011.
- [14] Y. P. Tong, S. B. Zhao, W. F. Feng, and L. Ma, "A study of Eu-doped $\text{La}_2\text{Zr}_2\text{O}_7$ nanocrystals prepared by salt-assistant combustion synthesis," *Journal of Alloys and Compounds*, vol. 550, pp. 268–272, 2013.
- [15] Y. P. Tong, S. B. Zhao, L. Ma, W. X. Zhao, W. H. Song, and H. Yang, "Facile synthesis and crystal growth dynamics study of MgAl_2O_4 nanocrystals," *Materials Research Bulletin*, vol. 48, no. 11, pp. 4834–4838, 2013.

